



Solution-processed white organic light-emitting devices based on small-molecule materials

Dongdong Wang^a, Zhaoxin Wu^{b,*}, Xinwen Zhang^b, Dawei Wang^b, Xun Hou^b

^a School of Science, Xi'an Jiaotong University, Xi'an 710049, PR China

^b Key Laboratory for Physical Electronics and Devices of the Ministry of Education, School of Electronic and Information Engineering, Xi'an Jiaotong University, Xi'an 710049, PR China

ARTICLE INFO

Article history:

Received 3 December 2008

Received in revised form

3 August 2009

Accepted 11 September 2009

Available online 30 September 2009

PACS:

85.60.Jb

78.60.Fi

78.66.Qh

Keywords:

White organic light-emitting devices

Solution processing

Organic small-molecule

ABSTRACT

We investigated solution-processed films of 4,4'-bis(2,2-diphenylvinyl)-1,1'-bibenyl (DPVBi) and its blends with N,N'-bis(3-methylphenyl)-(1,1'-biphenyl)-4,4'-diamine (TPD) by atomic force microscopy (AFM). The AFM result shows that the solution-processed films are pin-free and their morphology is smooth enough to be used in OLEDs. We have developed a solution-processed white organic light-emitting device (WOLEDs) based on small-molecules, in which the light-emitting layer (EML) was formed by spin-coating the solution of small-molecules on top of the solution-processed hole-transporting layer. This WOLEDs, in which the EML consists of co-host (DPVBi and TPD), the blue dopant (4,4'-bis[2-(4-(N,N-diphenylamino)phenyl)vinyl]biphenyl) and the yellow dye (5,6,11,12-tetraphenyl-naphthalene), has a current efficiency of 6.0 cd/A at a practical luminance of 1000 cd/m², a maximum luminance of 22500 cd/m², and its color coordinates are quite stable. Our research shows a possible approach to achieve efficient and low-cost small-molecule-based WOLEDs, which avoids the complexities of the co-evaporation process of multiple dopants and host materials in vacuum depositions.

© 2009 Elsevier B.V. All rights reserved.

1. Introduction

White organic light-emitting diodes (WOLEDs) are likely to play a major role in future lighting and backlight units for liquid crystal display due to their properties such as homogenous emission in a large area and flexible display. According to the report of D' Andrade and Forrest [1], for WOLEDs to gain wide acceptance in the general illumination market, the manufacturing costs must be < \$3 per 1000 lm. Therefore, finding a low-cost method to manufacture them is an important research goal. However, this target (< \$3 per 1000 lm) is difficult to realize with the vacuum-deposition method, although significant effort has been made in this direction.

In this paper, we demonstrate the fabricating small-molecule WOLEDs, whose hole-transporting layer (HTL) and light-emitting layer (EML) are fabricated by spin-coating. As is well known, small-molecule-based WOLEDs were extensively studied because we can dope one or more dopants into the host materials [2,3] or combining emission from different layers [4–6]. However, the process of doping two or more dopants into the host material by vacuum evaporation is quite complex and time-consuming, which

limits the commercial application of WOLEDs. In this respect, solution-processed WOLEDs are more desirable because they are compatible with low-cost and large-scale fabrication technology such as spin-coating, ink-jet printing and screen-printing [7].

Solution-processed WOLEDs have been extensively investigated in the past two decades, but the attention is primarily focused on polymer-based WOLEDs including single-layer [8–10] and multilayer structures [11,12]. However, although light-emitting polymers are considered to be suitable for solution printing, their performance is not sufficient in commercial WOLED devices. In contrast, the efficiency and lifetime of vacuum-deposited small-molecule WOLEDs significantly outperform those of polymer-based devices. Therefore, it is desirable to develop WOLED devices based on soluble small-molecules, which would combine performance of small-molecules with the low cost of solution processing. This would be a significant step toward the commercialized fabrication of WOLEDs. Since reports on the fabrication of small-molecule-based devices by means of solution processing are rare [13,14], it is our goal to demonstrate that this approach can indeed produce desired WOLEDs.

Four devices were fabricated in our experiments. In these devices, the composition of the EML is changed gradually from device 1 to device 4 to improve device performances and elucidate the advantages of the solution processing method in fabricating small-molecule WOLEDs, where co-doping of multiple dopants

* Corresponding author. Tel./fax: +86 29 82664867.

E-mail address: zhaoxinwu@mail.xjtu.edu.cn (Z. Wu).

and hosts is necessary. In device 1, the EML is based on blue emitter 4,4'-bis(2,2-diphenylvinyl)-1,1'-bibenyl (DPVBi) doped by yellow fluorescent dye 5,6,11,12-tetraphenylphtacene (rubrene). In devices 2 and 3, the EML consists of co-host of DPVBi and hole-transporting material N,N'-bis(3-methylphenyl)-(1,1'-biphenyl)-4,4'-diamine (TPD), and rubrene. In device 4, the EML consists of co-host (DPVBi and TPD), and the blue dopant 4,4'-bis[2-(4-(N,N-diphenylamino)phenyl)vinyl]biphenyl (DPAVBi) and rubrene. While these small-molecule WOLEDs have comparable current efficiency to that of vacuum-deposited devices based on the same light-emitting materials, the complexity of co-evaporation process and high costs are effectively avoided in our production process.

2. Experimental

The structures of the devices we built are summarized in Table 1. The poly(N-vinylcarboze) (PVK, Mw: 1100,000) or N,N'-bis(naphthalene-1-yl)-N,N'-bis(phenyl)-benzidine (NPB) doped PVK and the tris(8-hydroxyquinoline)aluminum (Alq₃) are used as HTL and electron-transporting layer (ETL), respectively. The 2,9-dimethyl-4,7-diaphenyl-1,10-phenanthroline (BCP) serves as the hole-blocking layer (HBL). The EML was spin-coated on top of the previously coated HTL. In producing multilayers by solution processing, the primary problem is to find a suitable solvent that does not damage or degrade the previously coated layers [15], such as PVK or NPB-doped PVK in this paper. The solvent p-xylene was used as a solvent for dissolving EML materials because p-xylene does not damage the PVK layer and only slightly dissolves the PVK:NPB (4:1) blending layer. On the other hand, it can effectively dissolve the organic materials used for EML.

In our experiment, PVK or PVK:NPB mixture was first dissolved in chlorobenzene, and the EML materials were then dissolved in p-xylene. A water-dispersed poly(3,4-ethylenedioxythiophene):polystyrene sulfonate (PEDOT/PSS) mixture was spin-coated on top of the patterned, pre-cleaned ITO-coated glass substrate to achieve film with a thickness of 35 nm, which was then baked at 138 °C for 30 min. In the next step, the HTL (40 nm) and EML with a thickness of 35 nm were spin-coated and baked at 90 °C for 40 min and at 80 °C for 30 min, respectively. Finally, the sample was loaded into the vacuum chamber to have the HBL, ETL and the cathode (LiF(0.6 nm)/Al(80 nm)) deposited by thermal evaporation.

The film thickness was measured by Ellipsometers. The CIE coordinates and electroluminescence (EL) spectra of the devices were measured by a spectrometer (PR650) and the current-voltage-luminescence characteristics were analyzed by a Keithley 2602 source meter. The devices for operational stability measurements were encapsulated, and measured using a constant dc current.

3. Results and discussion

The device performance of OLEDs is strongly affected by the morphology characteristic of the organic films [16]. Hence, the morphology of spin-coated layers as well as the ITO surface was investigated by AFM. Fig. 1 shows the AFM images of (a) bare ITO glass, spin-coated organic films of (b) PVK, (c) DPVBi on top of PVK, and (d) DPVBi:TPD (a weight ratio of 3:2) over PVK. As shown in Fig. 1(a) and (b), the films spun from PVK solution in chlorobenzene have a very smooth morphology with a 1.3 nm of root-mean-square (RMS) of surface roughness due to the good film-forming property of PVK (note: the RMS of surface roughness of ITO film is 1.5 nm) [17]. The AFM images in Fig. 1(c) and (d) indicate that spin-coated films of DPVBi and the blends of DPVBi:TPD were pin-free and smooth. Their surface roughness in terms of RMS was 1.2 and 1.8 nm, respectively. These images of AFM suggest that the small-molecule films fabricated by spin-coating were smooth enough to be used in the fabrication of OLEDs.

We now move to examine the performances of the WOLEDs we built. Fig. 2 depicts the (a) current density-voltage, (b) luminance-current density, (c) current efficiency-current density characteristics of devices 1–4, and Fig. 2(d) shows luminance decay versus time characteristic of device 4 at a constant current. In Fig. 2, device 4 employing blue dopant (DPAVBi) presents the best performance among the four devices. It shows a maximum luminance of 22500 cd/m² and a current efficiency of 6.0 cd/A at a practical luminance of 1000 cd/m². Device 3 with NPB in PVK exhibits better performances than device 2 without NPB in PVK. Device 3 has a maximum luminance of 9179 cd/m² and current efficiency of 4.5 cd/A (1000 cd/m²), while device 2 shows a maximum luminance of 5396 cd/m² and a current efficiency of 2.9 cd/A (1000 cd/m²), respectively. It can be seen that the device performances can be continuously improved by introducing TPD into EML, doping NPB into PVK or employing HIL(PEDOT/PSS) layer and using blue dopant DPAVBi with high emission efficiency. In Fig. 2(d), device 4 shows a half lifetime of 132 h at an initial luminance of 400 cd/m². The short device lifetime may be related to the low film density resulting from solution processing. It was recently demonstrated that a spin-coated film had lower film density than that of vacuum-deposited film by measuring the ordinary refractive index [18]. Therefore, obtaining denser molecular films by solution processing may help to improve the device lifetime. However, the effect of the density of the solution-processed small-molecule film on device lifetime needs to be further investigated.

In our experiments, introducing TPD into EML can both improve hole injection from the HTL to the EML and increase the hole transport in the EML. As shown in the energy-level diagrams of device 1 in Fig. 3(a), holes can directly enter the DPVBi molecules from HTL PVK in device 1. Upon the introduction of TPD, the holes can alternatively enter the EML via TPD

Table 1
Layer structures of the devices 1–4.

Device	HIL (nm)	HTL (40 nm)	EML(35 nm)			HBL (10 nm)	ETL (30 nm)
			Hosts	Rubrene (wt%)	DPAVBi (wt%)		
1		PVK	DPVBi	0.08		BCP	Alq ₃
2		PVK	DPVBi:TPD	0.08		BCP	Alq ₃
3		PVK:NPB	DPVBi:TPD	0.10		BCP	Alq ₃
4	PEDOT/PSS (35)	PVK:NPB(20 nm)	DPVBi:TPD	0.25	8	BCP	Alq ₃

Note: The doped concentration of DPAVBi is an optimized value range from 2% to 10% and the concentration of dyes in devices was determined against the weight of DPVBi or DPVBi:TPD, and the mixed ratio of PVK:NPB and DPVBi:TPD are 4:1 and 3:2, respectively.

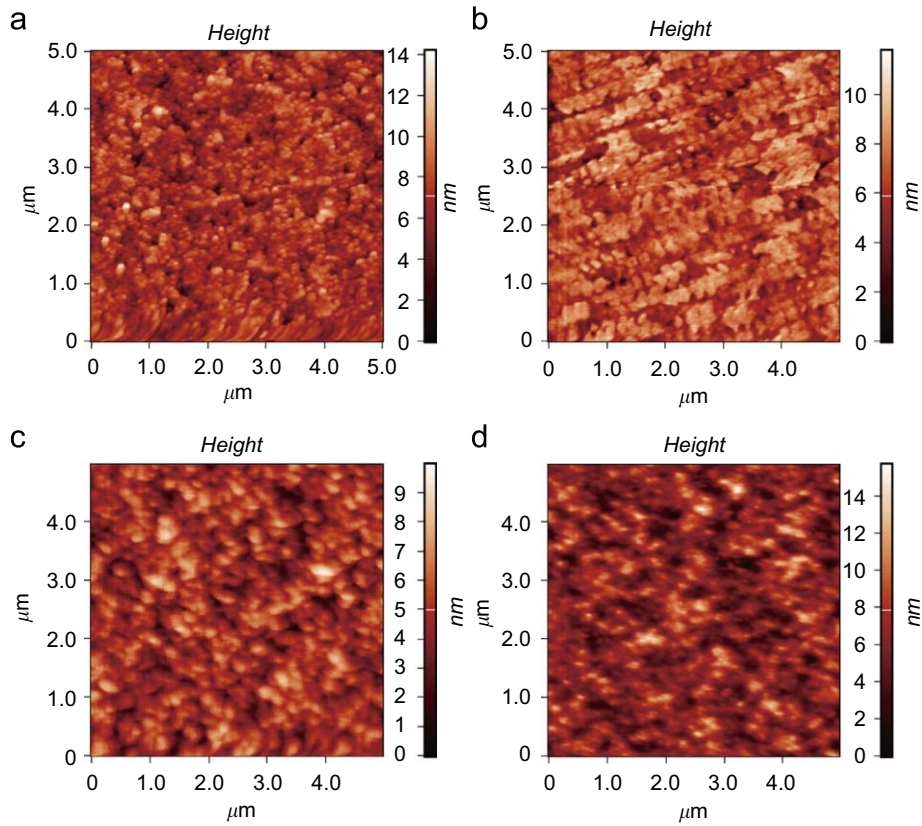


Fig. 1. AFM images of spin-coated organic films ($5\ \mu\text{m} \times 5\ \mu\text{m}$). (a) Bare ITO; R_{RMS} roughness = 1.5 nm. (b) Spin-coated film of PVK from chlorobenzene solution on ITO; $R_{\text{RMS}} = 1.3$ nm. (c) DPVBi spin-coated film from p-xylene solution on PVK; $R_{\text{RMS}} = 1.2$ nm. (d) Mixed film of DPVBi and TPD with a weight ratio of 3:2 spin-coated on PVK from p-xylene solution; $R_{\text{RMS}} = 1.8$ nm.

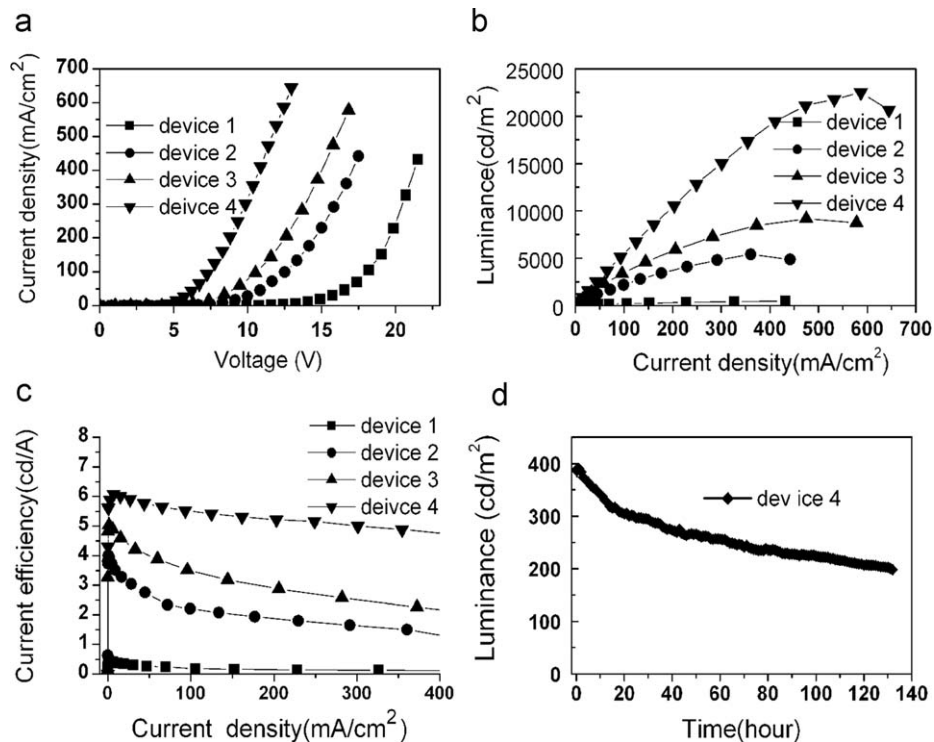


Fig. 2. (a) Current–voltage, (b) luminance–current density, (c) current efficiency–current density characteristic curves of devices 1–4 and (d) luminance decay versus time characteristic of device 4 at an initial luminance of $400\ \text{cd}/\text{m}^2$.

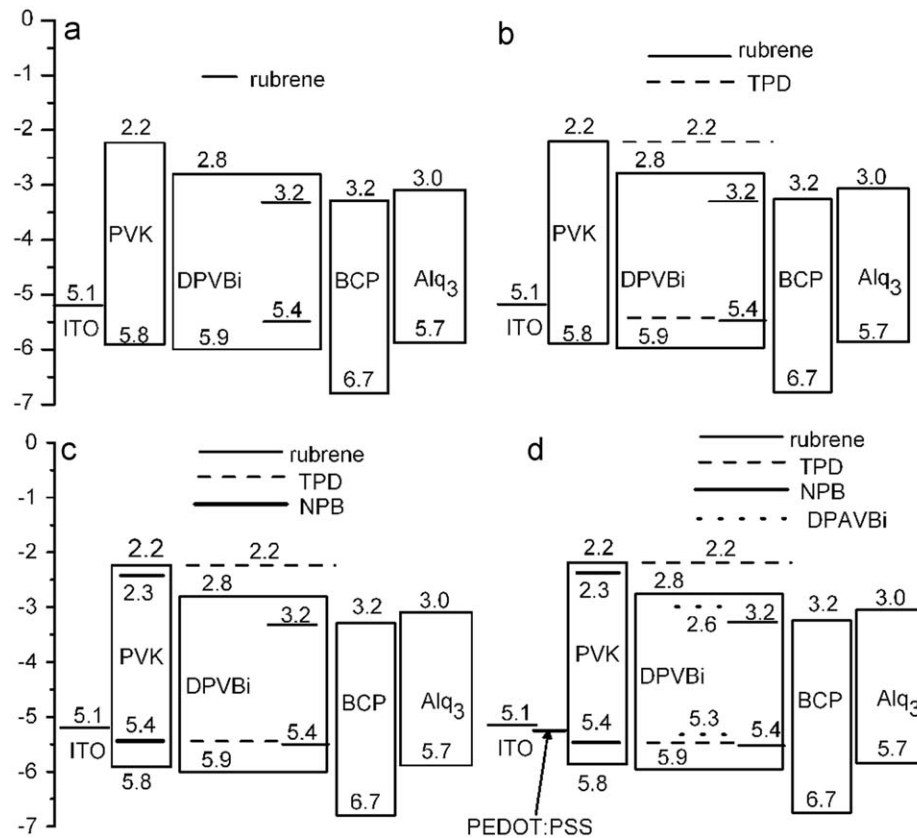


Fig. 3. (a)–(d) Schematic energy-level diagrams of devices 1–4.

molecules since the injection barrier from PVK to TPD is a negative value (-0.4 eV), while the injection barrier for holes to enter the DPVBi is 0.1 eV, as shown in Fig. 3(b). Upon the introduction of TPD, the hole transport of EML is also enhanced. Since the hole mobility of TPD ($1 \times 10^{-3} \text{ cm}^2 \text{ V}^{-1} \text{ s}^{-1}$) is several orders larger than that of DPVBi (about $10^{-7} \text{ cm}^2 \text{ V}^{-1} \text{ s}^{-1}$) [19,20], the holes entering the TPD are transported to the interface of EML/BCP quickly, leading to improved hole transport in the EML and enhanced carrier concentration close to the EML/BCP interface. Both factors help in generating more excitons, resulting in improved performance as a consequence.

The effect of NPB in HTL on device performances is also attributed to the improved hole transport in HTL and the increase of hole injection from the anode ITO to the HTL. The disadvantages of using PVK as HTL are its high hole-injecting barrier (0.7 eV for ITO/PVK interface) and the relatively low hole mobility (10^{-7} – $10^{-6} \text{ cm}^2 \text{ V}^{-1} \text{ s}^{-1}$) [21], which limit the improvement of device performance. The NPB is the most widely used hole-transporting materials, and it has a hole mobility of $10^{-4} \text{ cm}^2 \text{ V}^{-1} \text{ s}^{-1}$ [22] and a 0.2 eV interface energy barrier for hole injection, as shown in Fig. 3(c). Therefore doping of NPB into PVK can partially improve hole injection and transport in HTL. When 20% NPB was doped into PVK, the luminance and efficiency of our devices were significantly improved and were comparable with vacuum-deposited devices based on the same light-emitting materials [3,23]. However, the device performance still has room for improvement if we can dope highly efficient fluorescent dyes into the co-host of DPVBi and TPD. In device 4, we doped DPAVBi into the co-host of DPVBi and TPD, and obtained higher luminance and efficiency. This improvement mainly arises from the further enhanced hole injection, resulting from the use of PEDOT/PSS and the employment of DPAVBi, which has a higher fluorescent efficiency.

The stability of the CIE chromaticity coordinates is one of the critical parameters for the evaluation of white light sources. Fig. 4 shows the normalized EL spectra of (a) device 1, (b) device 2, (c) device 3 and (d) device 4 with various applied voltages. The CIE coordinates are shown in the inset. From Fig. 4(a)–(d), we see a significant increase in intensity with increase in voltage, but no obvious CIE shift. This result indicates that the CIE coordinates of our devices are independent of the applied voltages. As shown in the inset of Fig. 4(d), the color coordinates of device 4 changes only from $(0.312, 0.385)$ to $(0.316, 0.379)$ as the applied voltage increases from 4 to 12 V; the change of CIE coordinates are $(0.004, -0.006)$. Similarly, the CIE coordinates of device 3 vary from $(0.295, 0.339)$ at an applied voltage of 5 V to $(0.300, 0.354)$ at 13 V; the change of CIE coordinates is only $(0.005, 0.015)$. The stable color coordinates of our devices are attributed to the effective confinement of carriers in the EML and the suppression of hole-trapping due to rubrene molecules. The HBL, which is used to increase the recombination rate of electron–hole pairs, plays a significant role in confining the electron–hole pairs recombination close to the EML/BCP interface due to the hole-blocking effect of BCP. In devices 2–4, the TPD in the EML was employed to partially suppress the hole-trapping of rubrene molecules because the holes trapped on rubrene molecules can easily hop to the TPD since TPD and rubrene have the same highest occupied molecule orbital energy (5.4 eV) [24]. As we know, one of the major drawbacks for WOLEDs is the huge change of the CIE coordinates with the change in the applied voltage due to the recombination zone shift. However, the four devices avoided this drawback and exhibited highly stable white emission. We thus believe the production of the WOLEDs would benefit from a solution-based approach that allows functional materials such as TPD, DPAVBi to be used in the EML easily.

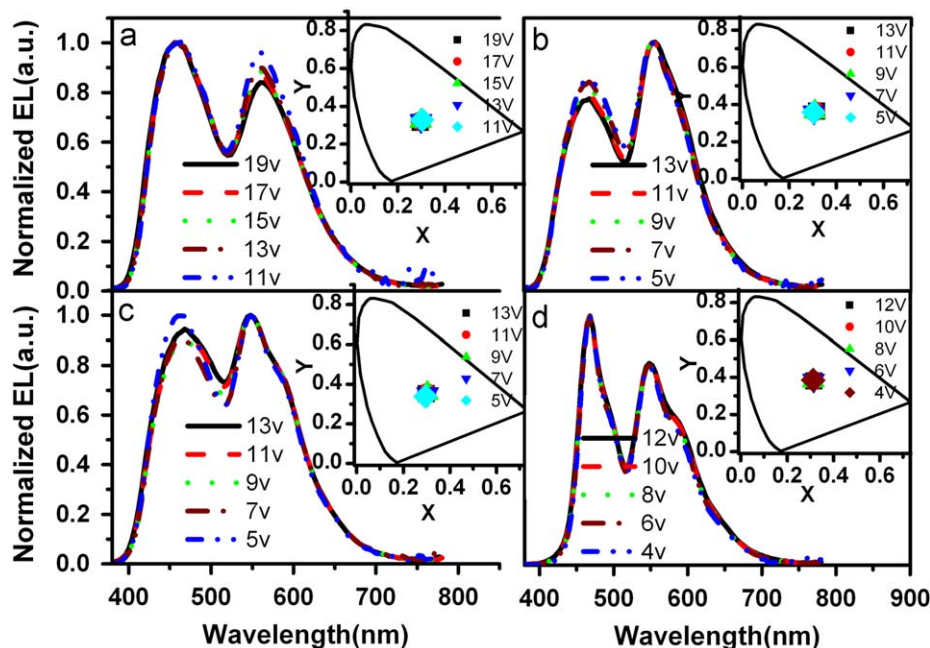


Fig. 4. Normalized EL spectra of (a) device 1, (b) device 2, (c) device 3 and (d) device 4 at different voltages, as well as CIE coordinates in the inset.

4. Conclusions

We have investigated the use of solution-based approach to produce organic thin films used in WOLEDs. The AFM results show that smooth films of DPVBi and blends of DPVBi and TPD can be achieved by spin-coating p-xylene solution. Based on spin-coated films, small-molecule WOLEDs were fabricated. Our research suggests that it is possible to use solution-processed small-molecule films for fabricating WOLEDs and the WOLEDs show a comparable performance to that of the vacuum-deposited devices. The solution-processing procedure, which is applied to small-molecule materials but not to polymers, readily provides for the precise co-doping of several dyes and the mixing of host materials and the complexity of co-evaporation process and high costs are effectively avoided.

Acknowledgments

The authors are grateful to Ministry of Science and Technology of China (973 program No. 2006CB921602), Ministry of Education of China (Key program No. 107100), Program for New Century Excellent Talents in University and the Technology Program of Shaanxi Province (No. 2006K04-c25) for financial support.

References

- [1] B. D'Andrade, S.R. Forrest, *Adv. Mater.* 16 (2004) 1585.
- [2] H.S. Yang, Y.W. Shi, Y. Zhao, J.Y. Hou, S.Y. Liu, *J. Lumin.* 127 (2007) 367.

- [3] X.Y. Zheng, W.Q. Zhu, Y.Z. Wu, X.Y. Jiang, R.G. Sun, Z.L. Zhang, S.H. Xu, *Displays* 24 (2003) 121.
- [4] X.F. Zhang, G. Cheng, Y. Zhao, J.Y. Hou, S.Y. Liu, *Appl. Phys. Lett.* 86 (2005) 011112.
- [5] H. Choukri, A. Fischer, S. Forget, S. Chénais, M.C. Castex, D. Adès, A. Siove, B. Geffroy, *Appl. Phys. Lett.* 89 (2006) 183513.
- [6] S.H. Yang, M.H. Liu, Y.K. Su, *J. Appl. Phys.* 100 (2006) 083111.
- [7] D.A. Pardo, G.E. Jabbour, N. Peyghambarian, *Adv. Mater.* 12 (2000) 1249.
- [8] J.S. Huang, G. Li, E. Wu, Q.F. Xu, Y. Yang, *Adv. Mater.* 18 (2006) 114.
- [9] J.S. Huang, W.J. Hou, J.H. Li, G. Li, Y. Yang, *Appl. Phys. Lett.* (2006) 133509.
- [10] X. Gong, S. Wang, D. Moses, G. Bazan, A.J. Heeger, *Adv. Mater.* (2005) 2053.
- [11] Y.H. Xu, J.B. Peng, J.X. Jiang, W. Xu, W. Yang, Y. Cao, *Appl. Phys. Lett.* 87 (2005) 193502.
- [12] G.K. Ho, H.F. Meng, S.C. Lin, S.F. Horng, C.S. Hsu, L.C. Chen, S.M. Chang, *Appl. Phys. Lett.* 85 (2004) 4576.
- [13] Y. Hino, H. Kajii, Y. Ohmori, *Org. Electron.* 5 (2004) 265.
- [14] N. Rehmman, D. Hertel, K. Meerholz, H. Becker, *Appl. Phys. Lett.* 91 (2007) 103507.
- [15] S.R. Forrest, *Nature* 428 (2004) 911.
- [16] M. Tomohiko, M. Takuya, I. Masahiko, H. Fujikawa, *Appl. Phys. Lett.* 80 (2002) 3895.
- [17] W.D. Gill, *J. Appl. Phys.* 43 (1972) 5033.
- [18] T.W. Lee, T.Y. Noh, H.W. Shin, O.Y. Kwon, J.J. Park, B.K. Choi, M.S. Kim, D.W. Shin, Y.R. Kim, *Adv. Funct. Mater.* 19 (2009) 1625.
- [19] M.V. der Auweraer, P.M. Borsenberger, F.C. De Schryver, H. Bassler, *Adv. Mater.* 6 (1994) 199.
- [20] E.I. Haskal, *Synth. Met.* 91 (1997) 187.
- [21] M.B. Khalifa, D. Vaufray, A. Bouazizi, J. Tardy, H. Maaref, *Mater. Sci. Eng. C* 21 (2002) 277.
- [22] S.L. Lai, M.Y. Chan, M.K. Fung, C.S. Lee, S.T. Lee, *Appl. Phys. Lett.* 90 (2007) 203510.
- [23] Y. Duan, Y. Zhao, G. Cheng, W.L. Jiang, J. Li, Z.J. Wu, J.Y. Hou, S.Y. Liu, *Semicond. Sci. Technol.* 19 (2004) L32.
- [24] C.H. Hsiao, C.F. Lin, J.H. Lee, *J. Appl. Phys.* 102 (2007) 094508.